RIELAC
Revista de Ingeniería Electrónica, Automática y Comunicaciones

Stride length estimation through the use of a single inertial sensor and the application of a method based on the detection of stability intervals

Fidel Hernández, Melissa Domínguez, Brenda Guitard, René Corvo, Jon Altuna

ABSTRACT / *RESUMEN*

The use of Inertial Measurement Units (IMUs) has emerged as a promising technique for estimating stride length during human gait. This research presents a new analytical approach to estimate this parameter. The estimation procedure is based on the identification and use of stability intervals before and after the swing phase of the sensor-mounted foot. The algorithm proposes attaching the inertial sensor to the forefoot. A database was built to validate the algorithm. The data were incorporated into the analysis gradually to gain insight into the sufficiency of the data used. Several metrics were computed, and the results revealed that the proposed algorithm exhibits a performance that outperforms the majority of the results reported by other studies to date.

Keywords: human gait; inertial sensor; stride length estimation; stability intervals

RESUMEN

El uso de Unidades de Medición Inercial (UMI) se ha convertido en una técnica prometedora para estimar la longitud de la zancada durante la marcha humana. Esta investigación presenta un nuevo enfoque analítico para estimar este parámetro. El procedimiento de estimación se basa en la identificación y el uso de intervalos de estabilidad antes y después de la fase de balanceo del pie con sensor. El algoritmo propone la fijación del sensor inercial al antepié. Se creó una base de datos para validar el algoritmo. Los datos se incorporaron gradualmente al análisis para comprender su suficiencia. Se calcularon diversas métricas y los resultados revelaron que el algoritmo propuesto presenta un rendimiento superior al de la mayoría de los resultados reportados en otros estudios hasta la fecha.

Palabras Claves: marcha humana; sensor inercial; estimación de la longitud de la zancada; intervalos de estabilidad

Estimación de la longitud de zancada mediante el uso de un único sensor inercial y la aplicación de un método basado en la detección de intervalos de estabilidad

1. -INTRODUCTION

The early evaluation of symptoms related to functional impairment allows for the early diagnosis of diseases and their possible complications, thus helping to determine the most appropriate treatment for each type of pathology [1]. The early detection of frailty in the elderly and the timely application of diagnostic, therapeutic, and rehabilitative techniques can positively impact their quality of life [2]. Several research works have been carried out to study the importance of physical performance indicators for classifying the functional capacity of elderly people. Among the most used parameters for evaluating physical performance are those related to gait [3].

Numerous strategies for gait evaluation have been proposed, leading to the identification of qualitative and quantitative criteria; however, quantitative evaluation strategies are the most developed, as they are objective, allow for a more complete assessment, and avoid observational errors [4]. Usually, laboratories for the study of human gait obtain spatiotemporal parameters simply through the use of measuring tapes, stopwatches, and systematic visual analysis performed by professionals [5].

Recibido: 10/2025 Aceptado: 02/2026

Among human gait parameters, stride length is one of the most important because it is related to movement efficiency and economy [6]. Furthermore, stride length can also be related to a person's posture and balance (e.g., an abnormal stride length can disrupt body alignment and increase the risk of injury or muscle imbalances) [6].

In recent years, various systems and equipment have emerged to obtain objective data for quantitative and effective gait evaluation through kinematics, dynamics, and other aspects such as the electrical activity of the muscles during movement [5]. In this sense, when this highly specialized technology is used for the analysis of clinical gait conditions, it is referred to as instrumented gait analysis. The most popular methods are those based on cameras, force platforms, or the use of portable sensors placed on various parts of the body [2].

An Inertial Measurement Unit (IMU) is capable of measuring position, orientation, and velocity [7]. Since this type of sensor does not require an external reference to obtain velocity and angular position, its fields of application are broad and diverse [8]. Such a device can be placed directly on specific locations of the body to understand joint kinematics [9]. Compared with other systems, the placement of these sensors does not require much time nor the involvement of experts in the process. IMUs placed on the lower limbs allow for gait analysis that is not restricted to laboratory conditions [9]. Despite the aforementioned advantages, the use of inertial sensors carries certain disadvantages, such as the inability to measure stride length directly [10].

In [11], an IMU, comprising three orthogonally oriented accelerometers, three gyroscopes, and three magnetometers, was attached to the participant's instep, and signal samples were acquired at 100 Hz. A position estimation algorithm was implemented based on the accumulation of foot displacements along the horizontal orientation. To detect steps, the authors applied two alternatives: one based on processing the angular velocity signals from the gyroscopes, and the other based on processing the magnetic field signals from the magnetometers. The method exhibited a relative error of around 5%.

In [12], a study focused on extracting each individual stride length using an easy-to-use algorithm that required only one inertial sensor attached to the subject's shank. The mean relative error was lower than 6% for the healthy group and 10.3% for the Parkinson's disease group.

A deep learning-based step length estimation model, adaptable to different phone carrying positions and requiring neither individual stature information nor constrained spatial conditions, was proposed in [13]. This method achieved a mean relative error of 3.01%.

Wang and colleagues [14] combined smartphone mode recognition with stride length estimation to provide an accurate walking distance estimation. They applied multiple classification models to recognize five smartphone modes (calling, handheld, pocket, armband, swing). In addition to using a combination of time-domain and frequency-domain features from the built-in accelerometers and gyroscopes during the stride interval, higher-order features were constructed based on established studies to model stride length using a machine learning regression model. The mean absolute error and relative error were 0.036 m and 3.04%, respectively.

In [15], a stride-length estimation method based on a long short-term memory network and denoising autoencoders was presented. This method achieved a stride-length error rate of 4.59% and a mean absolute error of 0.058 m.

A single convolutional neural network model to predict the stride length of running and walking and to classify the running or walking type per stride was proposed in [16]. The model trains its pretext task using self-supervised learning on a large unlabeled dataset for feature learning, and its downstream task on the stride length estimation and classification tasks using supervised learning with a small labeled dataset. The proposed model achieved a mean relative error and a mean absolute error of 7.44% and 0.062 m, respectively, for stride length estimation.

In [17], a step length estimation model that utilizes acceleration magnitude was presented. The model was constructed by applying principal component analysis to data collected from anatomical landmarks on the human body during walking, using a highly accurate optical measurement system. The performance of the proposed model was evaluated for four typical smartphone positions for long-term human walking, producing an overall mean absolute stride length estimation error of 0.064 m.

A study presented in [18] aimed to develop an improved foot trajectory and stride length estimation method for level-ground running based on foot displacement. The accelerations and angular velocities of the left and right feet were measured with two IMUs mounted on the dorsum of each foot. In this study, foot trajectories between two consecutive and ipsilateral midstance instances were estimated using two methods: (1) a spatial error-correcting algorithm and (2) a velocity-based linear dedrifting technique. For different running velocity categories, the best mean absolute error was 0.05 m.

A study addressing an artificial intelligence-empowered and cost-effective gait monitoring system was presented in [19]. A pair of intelligent shoes with a single inertial sensor and a smartphone application were developed as a gait monitoring system

to detect the user's gait cycle, stand phase time, swing phase time, stride length, and foot clearance. This paper applied an Extreme Learning Machine algorithm for stride length estimation. The Vicon motion capture system was used to verify the accuracy of the gait metrics, and the results exhibited an RMSE of 0.0184 m.

Several machine-learning models to estimate step length based on data from a single lower-back inertial measurement unit worn by subjects with different neurological conditions, including Parkinson's disease and healthy controls, were developed and presented in [20]. For a single step, the best model showed an RMSE of 0.0608 m.

In summary, the approaches implemented for stride length estimation are primarily based on analytical methods or the application of machine learning techniques. Most analytical approaches usually require dealing with inherent problems, such as the projection of the gravity acceleration vector on the three IMU axes and the gyroscope signal drift; together, these major issues affect task performance. On the other hand, machine learning techniques can overcome these drawbacks; however, the performance of the resulting models can be degraded when the method must process data not included in the validation database [13].

This work proposes an analytical method for stride length estimation. This method leverages the stability intervals that occur during the gait cycle for acceleration and velocity initialization and implements a new approach for rotation angle adjustment to minimize the drift effect.

2.- MATERIALS AND METHODS

2.1.- PROPOSED ALGORITHM

Existing algorithms have exhibited significantly low effectiveness due to drift, vibration sensitivity, sensor limitations, and inaccurate integration with other systems [10]. This work proposes a new algorithm to obtain more accurate and reliable position estimates. Similar to the basic approach applied for stride length estimation, this algorithm is based on the analysis of IMU signals within the interval corresponding to the swing phase of the foot carrying the sensor. Consequently, the first step focuses on detecting the stability intervals that precede and follow the swing phase.

2.1.1.- DETERMINATION OF THE PRECEDING AND FOLLOWING STABILITY PHASE INTERVALS

To determine the stability intervals preceding and following the swing phase of the foot carrying the sensor, the longitudinal acceleration signal is proposed for use. This signal best represents the ascent and descent of the foot during the swing phase; it was therefore assumed that it could reveal the stability intervals more clearly. The analysis then focuses on identifying the extreme points—the points of starting stability (SSP) and ending stability (ESP)—which correspond to the preceding and following stability intervals around each swing phase. Figure 1 shows an example of a longitudinal acceleration signal from an IMU mounted on the forefoot during gait.

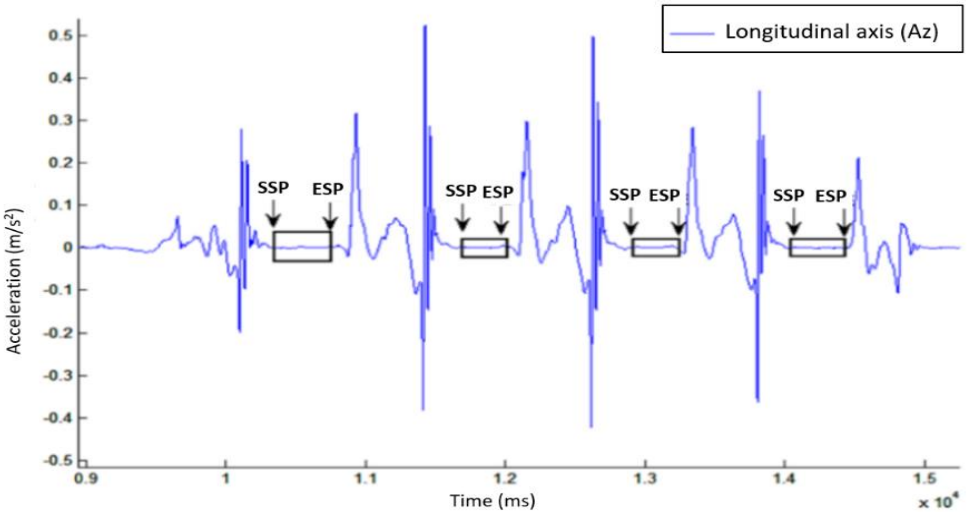

Figure 1

Example of longitudinal acceleration signal (IMU mounted at the forefoot) during a gait. Points of starting stability and ending stability, SSP and ESP.

The ESPs are determined by computing the variance of a 0.4 s moving window (shifting from left to right). The ending points of every set of consecutive windows with a variance below 0.8 m^2/s^4 (a threshold selected after a detailed empirical study of the database signals) are identified as the ESPs.

The SSPs are determined by computing the variance of a 0.2 s window that moves from each ESP to the left. The ending point of a set of consecutive windows with a variance below 0.5 m^2/s^4 (similar to the ESP detection, this threshold was selected after a detailed empirical study of the database signals) is identified as an SSP.

Having identified the stability intervals, the next step is to estimate the distance traveled by the foot in the anteroposterior direction between these intervals; that is, the stride length.

2.1.2.- ESTIMATION OF THE ANTEROPOSTERIOR DISPLACEMENT OF THE IMU-MOUNTED FOOT BETWEEN CONSECUTIVE STABILITY INTERVALS

As previously mentioned, the interval between the stability intervals is used to estimate the distance traveled by the foot. However, the proposed algorithm also uses the information within both the preceding and following stability intervals. These intervals are used to perform adjustments to the estimated parameters, as will be explained later. In this algorithm, the preceding stability interval is divided into two equal-length subphases: subphase 1 and subphase 2 of the preceding stability interval (see Figure 2).

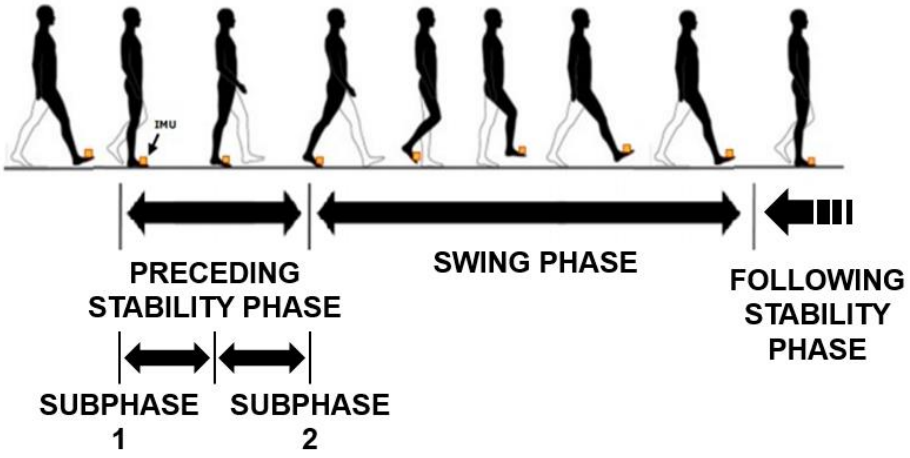

Figure 2

Example of longitudinal acceleration signal (IMU mounted at the forefoot) during a gait. Points of starting stability and ending stability, SSP and ESP.

A diagram of the proposed algorithm is shown in Figure 3. The procedure for estimating a single stride length using signals from an IMU placed on the forefoot is carried out as follows:

1. Using the signals from the 3D accelerometer and the 3D magnetometer, the rotation angles within subphase 1 of the preceding stability phase and the following stability phase intervals are determined. These angles represent the initial and final orientation of the inertial sensor during a stride execution. They are commonly known as Euler angles: roll (ϕ), pitch (θ), and yaw (ψ), as shown in Figure 4. These angles constitute a set of three angular coordinates that define the orientation of the system relative to a reference frame. This calculation involves the signals from the accelerometers and magnetometers and is performed using the following equations:

$$\phi = \tan^{-1}\left(\frac{A_Y}{\sqrt{{A_X}^2 + {A_Z}^2}}\right) \quad (1)$$

$$\theta = \tan^{-1}\left(\frac{A_X}{\sqrt{{A_Y}^2 + {A_Z}^2}}\right) \quad (2)$$

$$\psi = \tan^{-1}\left(\frac{B_y}{B_x}\right) \quad (3)$$

where A_X, A_Y, and A_Z are the signals from the IMU's accelerometers, and B_Y and B_X are the magnetic field measurements on the Y and X axes, respectively.

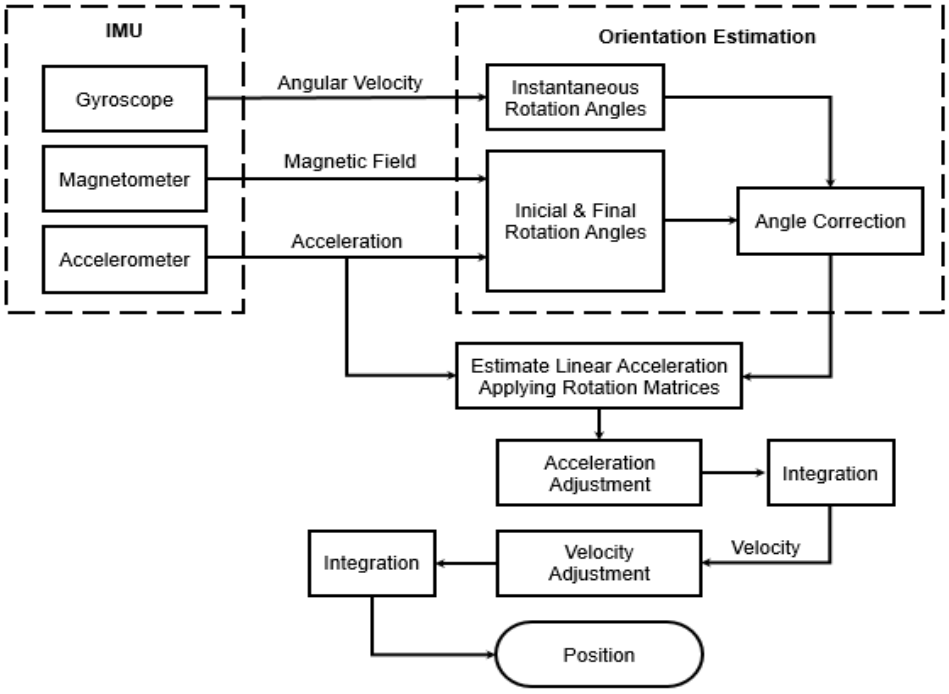

Figure 3

Diagram of the proposed algorithm.

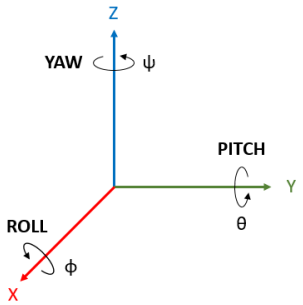

Figure 4

Rotation angles representation.

2. The IMU's rotation angles are determined using the 3D gyroscope signals within the interval comprising subphase 2 of the preceding stability phase, the swing phase, and the following stability phase.

   To reduce the impact of drift, a correction is applied to the angle measurements within the interval covering subphase 2 of the preceding stability phase, the swing phase, and the following stability phase. This correction ensures that the average value of the rotation angles within the following stability phase—estimated from the 3D gyroscope signals—approximates those estimated using the 3D accelerometer and 3D magnetometer. The correction consists of applying a linear variation to the angle values equal to $\frac{n}{N}\Delta$, where nn is the sample number and Δ is a parameter chosen such that the mean of the rotation angles within the following stability interval (estimated from the gyroscope signals) equals the mean of the rotation angles estimated from the 3D accelerometer and the 3D magnetometer. The value of Δ is calculated as follows (see Appendix A):

$$\Delta = \frac{\sum_{k=P+M+1}^{N} ang_g(k) \; - \; L \cdot FinalAngle_{MeanValue}}{\sum_{k=P+M+1}^{N} \frac{k}{N}} \tag{4}$$

   where $ang_g(k)$ is the value of sample k of the rotation angle obtained from the corresponding gyroscope signal; $FinalAngle_{MeanValue}$ is the mean of the rotation angles within the following stability interval, estimated from the 3D accelerometer and 3D magnetometer; P is the number of samples in subphase 2 of the preceding stability phase; M is the number of samples in the swing phase; and L is the number of samples in the following stability phase.

3. By applying a rotation to the IMU's coordinate axes, the gravity vector components are removed from the 3D accelerometer signals. For the rotation procedure in the interval covering subphase 2 of the preceding stability phase and the swing phase, the rotation angles estimated by the 3D gyroscope in Step 2 are used. For the rotation procedure in the interval corresponding to the following stability phase, the rotation angles estimated by the 3D accelerometer and the 3D magnetometer in Step 1 are used. The following rotation matrices are applied [21]:

$$R_x(\phi) = \begin{bmatrix} 1 & 0 & 0 \\ 0 & \cos\phi & -\sin\phi \\ 0 & \sin\phi & \cos\phi \end{bmatrix} \tag{5}$$

$$R_y(\theta) = \begin{bmatrix} \cos\theta & 0 & \sin\theta \\ 0 & 1 & 0 \\ -\sin\theta & 0 & \cos\theta \end{bmatrix} \tag{6}$$

$$R_z(\psi) = \begin{bmatrix} \cos\psi & -\sin\psi & 0 \\ \sin\psi & \cos\psi & 0 \\ 0 & 0 & 1 \end{bmatrix} \tag{7}$$

   Several Euler angle conventions exist to define rotation matrices, differing in the sequence of rotations around the three coordinate axes. The selected convention is ZYX, commonly used in orientation and position estimation applications, and is given by the following equation:

$$R_{rot} = R_z(\psi) \cdot R_y(\theta) \cdot R_x(\phi) \tag{8}$$

   The resulting rotation matrix is multiplied by the vector formed by the X, Y, and Z components of the acceleration signal obtained directly from the 3D accelerometer, yielding new, rotated acceleration components.

4. The double integration of the rotated acceleration signals would, in principle, result in the displacement signal. However, since the effect of drift on the rotation angle estimation is not completely removed, the velocity estimated by integrating the acceleration signals, and the subsequent displacement estimated from this velocity, will not be optimal. Therefore, a two-step adjustment is proposed: first on the rotated acceleration signals, and then on the velocity signals resulting from integrating the adjusted accelerations.

   a. For the interval covering both the swing phase and the following stability phase, a forward linear adjustment equal to $\frac{n}{N_{a_1}}\Delta_{a_1}$ is applied to the samples of the signal being adjusted, where n is the sample index and N_{a_1} is the total number of samples in the interval. A schematic showing the arrangement of the samples and their corresponding indices is presented in Figure 5 (this figure uses a fictitious signal for illustrative purposes). This first adjustment ensures that the average of the samples within the following stability phase—which will be processed by the subsequent integration—is equal to zero. This zero-average condition is based on

the assumption that, within a stability interval, the values for both acceleration and velocity should be zero. The parameter Δ_{a_1} is determined as follows (see Appendix B):

$$\Delta_{a_1} = \frac{\sum_{k=M+1}^{N_{a_1}} SignalToInt(k)}{\sum_{k=M+1}^{N_{a_1}} \frac{k}{N_{a_1}}} \tag{9}$$

where $SignalToInt(k)$ is the value of sample k of the signal (acceleration or velocity) to be adjusted, and M is the number of samples within the swing phase.

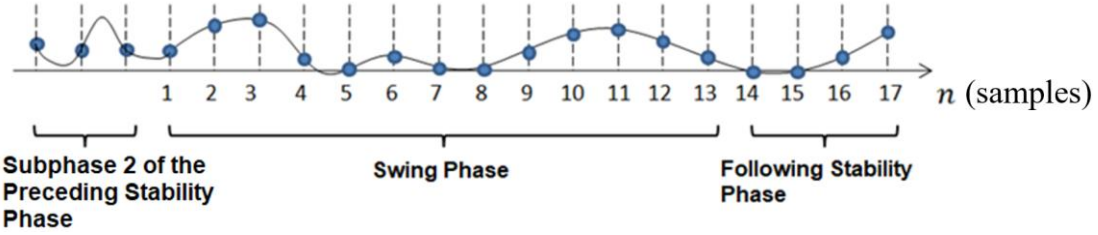

Figure 5

Example of sample numbering for the forward adjustment applied.

b. For the interval covering both subphase 2 of the preceding stability phase and the swing phase, a backward linear adjustment equal to $\frac{n}{N_{a_2}}\Delta_{a_2}$ is applied to the samples of the signal that were previously adjusted in the forward manner. Here, n is the sample index and N_{a_2} is the total number of samples in this interval. This second adjustment ensures that the average of the samples within subphase 2 of the preceding stability phase—which will be processed by the subsequent integration—is equal to zero. This condition is based on the assumption that, within a stability interval, the values for both acceleration and velocity should be zero.

In this backward adjustment, the samples are processed in reverse order. The sample with index $n = 1$ corresponds to the last sample of the swing phase, and the sample with index $n = N_{a_2}$ corresponds to the first sample of subphase 2 (see Figure 6). The parameter Δ_{a_2}, determined using the same principles as Δ_{a_1}, is calculated as follows:

$$\Delta_{a_2} = \frac{\sum_{k=M+1}^{N_{a_2}} Adj_{Signal(k)}}{\sum_{k=M+1}^{N_{a_2}} \frac{k}{N_{a_2}}} \tag{10}$$

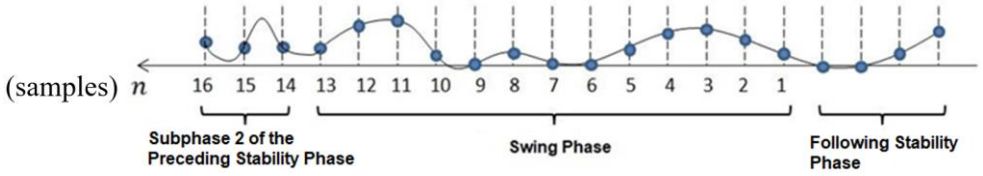

Figure 6

Example of sample numbering for the backward adjustment applied.

5. After applying this two-step adjustment to the rotated acceleration signals, a first integration is performed on the resulting signals over the interval covering subphase 2 of the preceding stability phase, the swing phase, and the following stability phase. The result is the velocity signal. Next, a second two-step adjustment is applied to the velocity signal, followed by its integration over the same interval. The final outcome is the displacement signal.

2.2.- EXPERIMENT AND VALIDATION

The validation of the algorithm proposed in Section IV is presented in this section. A database comprising IMU signals collected during experimental trials was constructed for this purpose. In the experimental setup, participants walked along a runway featuring equidistant guidelines spaced at 0.01 m intervals (see Figure 7). A single IMU was placed on the forefoot

(see Figure 8). Three video cameras were positioned along and beside the runway to obtain reference stride length measurements.

Figure 7

Walking across the runway.

Figure 8

IMU placement location.

The IMU-based wearable device used in this research was developed by the Signal Processing Applications Group (GAPS) at Cujae University and the Cuban Center for Neuroscience. The device incorporated an InvenSense MPU-92/65 sensor and was designed to transmit digitized IMU signals to a computer via Bluetooth. The MPU-92/65 is a 9-axis motion and orientation sensor that combines an accelerometer, gyroscope, and magnetometer on a single chip, providing measurements along all three axes (X, Y, Z). A sampling frequency of 1 kHz was used during the tests.

Accelerometer, gyroscope, and magnetometer signals were recorded while each subject walked a 5-meter path along the runway. The 30 subjects involved in the measurements—healthy men and women aged between 18 and 35 years—provided informed consent prior to their participation. The study was conducted in accordance with the Declaration of Helsinki, and the protocol was approved by the Scientific Committee of the Faculty of Telecommunications and Electronics.

In this work, the stride length estimation algorithm was validated using the constructed dataset. The following performance metrics were employed:

- the mean absolute error,

$$E_{abs} = \sum_{i=1}^{N} \frac{|\, x_i - \hat{x}_i|}{N} \tag{11}$$

- the mean relative error,

$$E_{rel} = \frac{1}{N} \sum_{i=1}^{N} \frac{|\, x_i - \hat{x}_i|}{x_i} \tag{12}$$

- the RMSE value,

$$RMSE = \sqrt{\frac{\sum_{i=1}^{N} |x_i - \hat{x}_i|^2}{N}} \tag{13}$$

- the coefficient of determination,

$$R^2 = 1 - \frac{\sum_{i=1}^{N}(x_i - \hat{x}_i)^2}{\sum_{i=1}^{N}\left(\hat{x}_i - \bar{\hat{x}}\right)^2} \tag{14}$$

where x_I is the reference stride length, $\hat{x}_I$ is the estimated stride length, N is the number of stride realizations, and $\bar{\hat{x}}$ is the average of the N predicted values.

Despite being less conventional, the coefficient of determination R^2 was employed because it allows for a global assessment of the quality and consistency of the estimation algorithm. This index represents the percentage of variability observed in the measured values that is captured by the estimation algorithm. An R^2 value close to 100 % means that the estimated stride length values closely follow the behavior of the measured real values.

To assess the consistency of the results, E_{abs}, E_{rel}, $RMSE$ and R^2 were computed by gradually including data in the analysis, one stride at a time. This approach allows for observing the stabilization of the metrics' trends, indicating when the amount of analyzed data can be considered sufficient and the results deemed reliable. No more than 100 stride realizations were needed to achieve this stabilization.

Because the Shapiro-Wilk test [22] indicated that the algorithm's measurement errors were not normally distributed, non-parametric tests were employed to evaluate its performance. The following statistical tests and inference methods were used:

- Wilcoxon Signed-Rank Test [23]: Applied to detect whether the algorithm showed a consistent tendency to overestimate or underestimate stride length. This test evaluates whether the median of the differences between the true and estimated measurements differs significantly from zero (H_0: $Median = 0$), considering both the sign and relative magnitude of the errors.
- Intraclass Correlation Coefficient (ICC) [24]: Applied to assess the agreement between the algorithm and the reference method, specifically using the 3,1 model. This index measures the degree of absolute agreement between two measurement methods, taking into account both between-subjects variability and error variability (H_0: $ICC = 0$).
- Bland-Altman Analysis [24]: Applied to characterize the overall behavior of the error, including its magnitude and dispersion. This analysis uses the median as the bias estimator and percentiles as limits of agreement.
- Bootstrap Confidence Intervals [25]: Applied to estimate 95% confidence intervals for the E_{abs} and $RMSE$ metrics using a Bootstrap resampling procedure. This method allows for assessing the stability of the metrics against sample variations without assuming any specific distribution for the error.

3.- RESULTS AND DISCUSSION

Two examples of the results from applying the procedure to determine the preceding and following stability phase intervals are shown in Figure 9. This figure shows the detected SSPs and ESPs with vertical magenta and green lines, respectively. It can be observed that an SSP-ESP pair is detected on both sides of each swing phase of the foot carrying the IMU. Both signals correspond to the Z-axis acceleration of the inertial sensor attached to the forefoot. Figures 9a and 9b show acceleration signals acquired from subjects who took 5 and 3 steps, respectively, with the instrumented foot. In both cases, a preceding and a following stability interval were successfully detected for each individual step.

Figure 10 presents the results of applying the displacement estimation algorithm to the steps shown in Figure 9. Figures 10a and 10b depict the estimated displacement signals corresponding to the sequences of 5 and 3 steps, respectively.

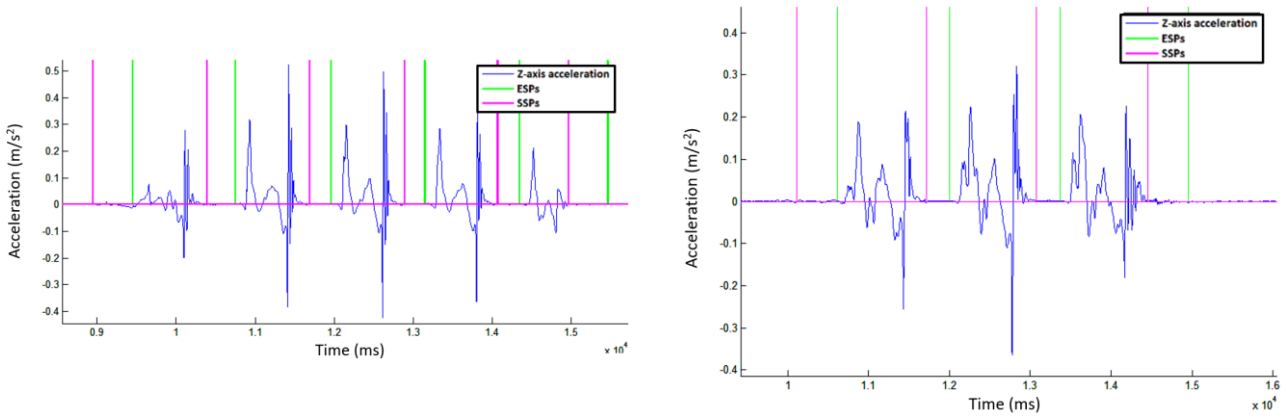

a) b)

Figure 9

Samples of the results achieved from the application of the procedure for determination of the preceding and following stability phase intervals (SSPs and ESPs detection): (a) 5 and (b) 3 steps with the IMU-mounted foot (Z-axis accelerations of the inertial sensor attached to the forefoot of the foot).

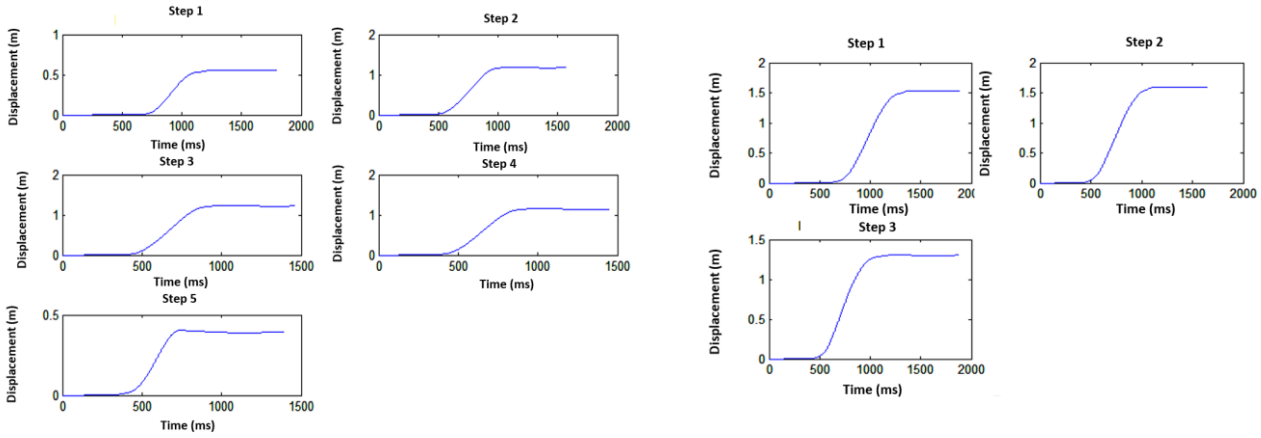

a) b)

Figure 10

Samples of displacement signals estimated by the algorithm. a) Displacement signals corresponding to 5 steps. b) Displacement signals corresponding to 3 steps.

The total displacement signal, representing the total traveled distance, can be reconstructed by concatenating the individual displacement signals estimated between stability intervals. Figure 11 shows (blue line) the total displacement signals synthesized from the individual step displacements shown in Figure 10. Figures 11a and 11b show the total displacement signals corresponding to the sequences of 5 and 3 steps, respectively. In Figure 11, the red line represents the reference (true) value of the traveled distance.

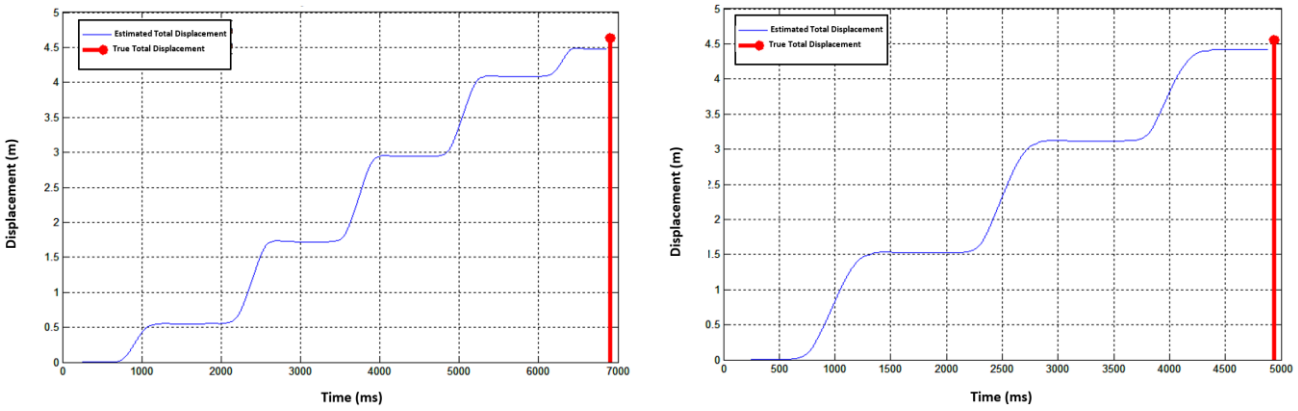

Figure 11

Total displacement signals synthetized from the displacement signal corresponding to the single steps shown in Figure 10. a) Total displacement signal corresponding to 5 steps. b) Total displacement signal corresponding to 3 steps.

The proposed algorithm was validated using the IMU signals database and the metrics, statistical test and inference methods defined in Section V. As previously explained, the algorithm was applied to a data subset that was gradually increased to ensure the reliability of the outcomes. The trends of E_{abs} and $RMSE$ are shown in Figure 12, and the trends of E_{rel} and R^2 are shown in Figure 13. These figures demonstrate that the metrics stabilize for data from 80 realizations onward. Therefore, the amount of processed data can be considered sufficient to deem the results reliable. The final values obtained were: $E_{abs} = 0.031\ m$, $RMSE = 0.0412\ m$, $E_{rel} = 2.82\ \%$, and $R^2 = 98.28\ \%$.

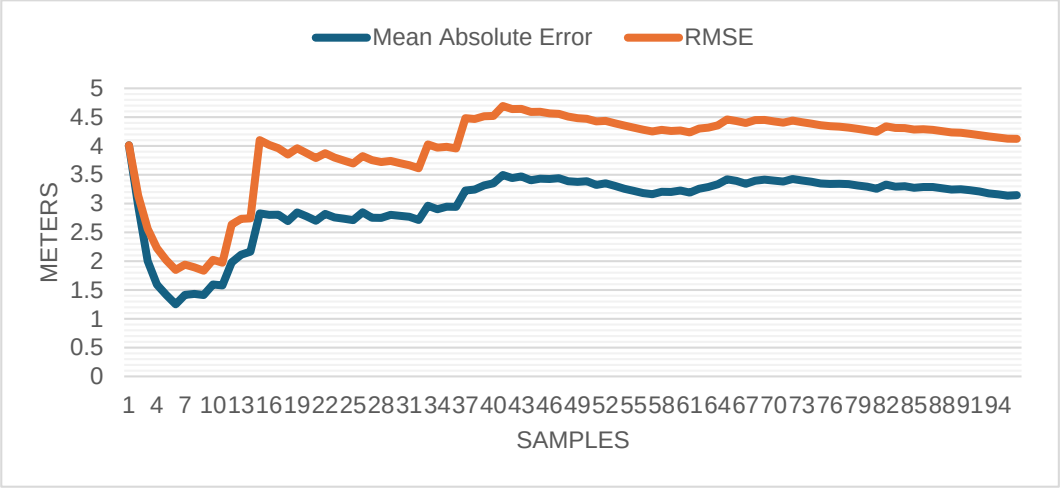

Figure 12

Trends of the series of E_{abs} and $RMSE$ values.

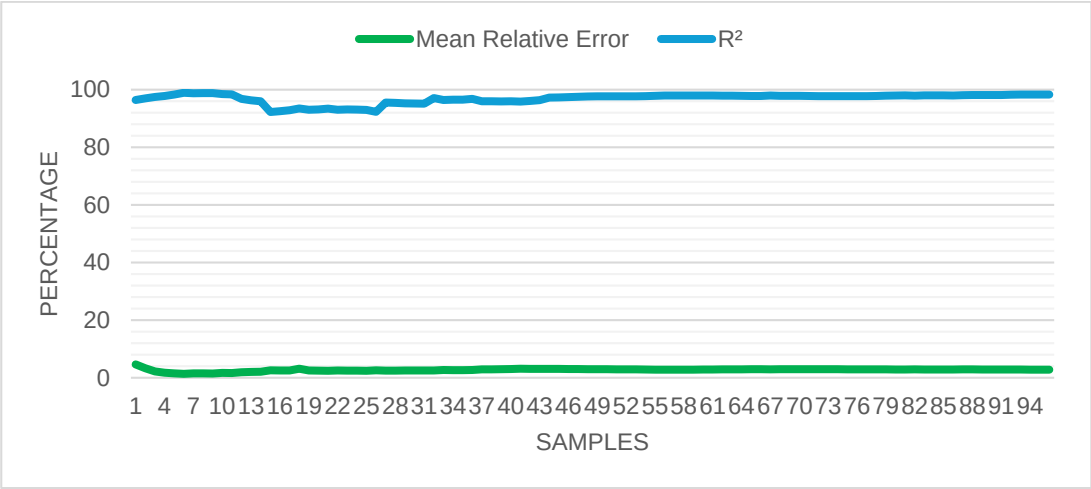

Figure 13

Trends of the series of E_{rel} and R^2 values.

To provide a qualitative comparison between the true stride lengths and the corresponding estimates from the algorithm, these values are presented in Figure 14. In this figure, the two sets of values—true stride lengths (blue) and estimated stride lengths (red)—are plotted after sorting the true values in increasing order. This graphical representation offers a qualitative assessment of the algorithm's effectiveness, showing that the estimated values closely match the true ones, thus demonstrating the algorithm's high accuracy.

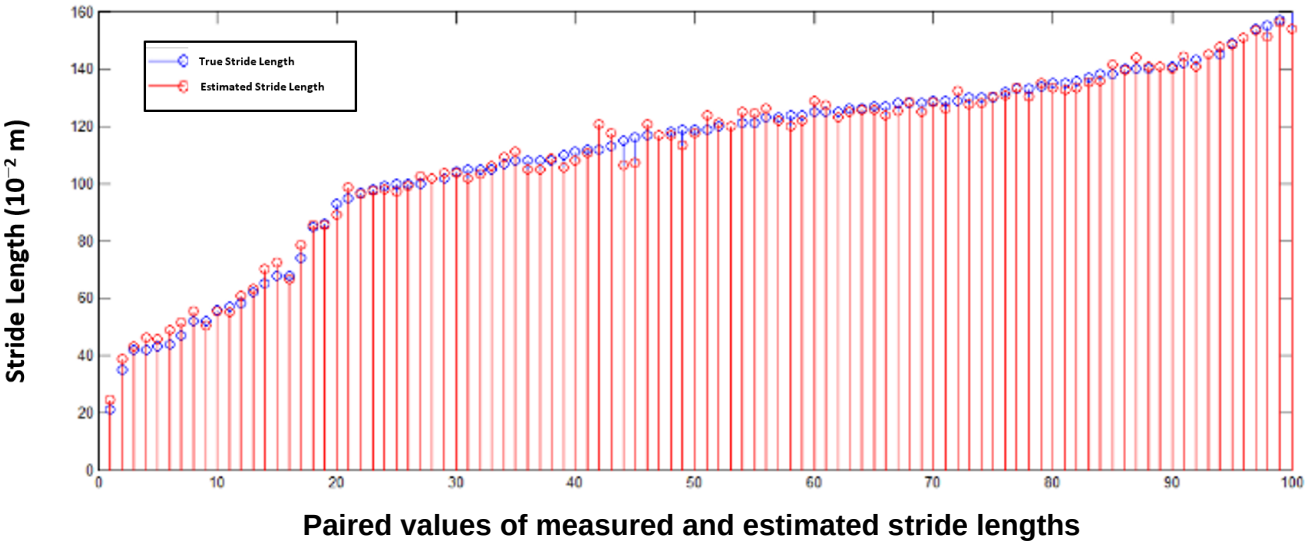

Figure 14

True and estimated stride lengths.

The results obtained from the proposed algorithm were compared with those from other research works, as presented in Table 1. The table shows that the proposed algorithm outperforms the majority of the results reported in previous studies. The RMSE from the method presented in [19] is the only metric that performed slightly better than the value achieved in this work. In [19], a high-performance, artificial intelligence-empowered gait monitoring system was developed. However, it is important to note that while AI-based approaches offer versatility, their performance can degrade when analyzing subjects whose walking characteristics differ significantly from those represented in the training dataset [13].

Table 1
Comparison of the performance achieved by the proposed algorithm with those achieved by previously developed algorithms

Algorithm	Mean absolute error (m)	Mean relative error (%)	RMSE (m)	R^2 (%)
Jimenez, 2009 [11]	-	5	-	-
Sijobert, 2015 [12]	-	6	-	-
Gu, 2019 [13]	-	3.01	-	-
Wang, 2019 [14]	0.036	3.04	-	-
Wang, 2020 [15]	0.058	4.59	-	-
Sui, 2021 [16]	0.062	7.44	-	-
Vezocnik, 2021 [17]	0.064	-	-	-
Suzuki, 2022 [18]	0.050	-	-	-
Zhou, 2024 [19]	-	-	0.0184	96.17
Zadka, 2024 [20]	-	-	0.0608	-
Proposed algorithm	**0.031**	**2.82**	**0.0412**	**98.28**

As previously mentioned, several statistical tests and inference methods were applied. The Wilcoxon Signed-Rank Test yielded a probability value of $p = 0.3965$, indicating insufficient evidence to reject the null hypothesis that the median of the differences is zero. Therefore, the estimated values are close to the true values without a directional trend. This points to an absence of systematic bias in the algorithm, demonstrating the method's accuracy. Furthermore, the obtained ICC was 0.9913. As this value significantly exceeds the common threshold of 0.90, there is sufficient evidence to reject the null hypothesis that the $ICC = 0$. According to established reliability criteria, values above 0.90 represent excellent agreement. This demonstrates a nearly perfect agreement between the estimated and actual measurements, evidencing the algorithm's high precision and stability in estimating stride length. This result suggests the possibility of replacing the true values with those estimated by the algorithm.

The Bland-Altman analysis identified a median difference of 0.0015 m, which aligns with the Wilcoxon test result, and a variability range marked by agreement limits of -0.1098 m (lower) and 0.0625 m (upper), as shown in Figure 15. This analysis reveals no systematic bias—confirming the algorithm's accuracy in agreement with the Wilcoxon test—but it does show notable dispersion and moderate variability in the extreme differences. This dispersion is consistent with the high precision and stability of the estimates indicated by the obtained ICC. Finally, the 95 % Bootstrap confidence intervals for the E_{abs} and $RMSE$ metrics were $[0.0262\text{ m}, 0.0369\text{ m}]$ and $[0.034\text{ m}, 0.0483\text{ m}]$, respectively. Given that these intervals are narrow and that the calculated point metrics fall within their bounds, it can be concluded that these metrics are robust and reproducible.

3.1.- A DEEPER ANALYSIS OF THE RESULTS

In this work, a more detailed analysis was performed on the resulting estimations, particularly those that showed significant deviation from the corresponding true stride length values. The study determined that in most cases, the poorest results corresponded to the stride length estimation of the first step. The authors consider that this is related to the movement dynamics of a subject transitioning from a static position to motion. Presumably, this initial action establishes dynamics with particular characteristics compared to the subsequent steps taken once the subject is already in motion. The most critical evidence of this phenomenon was the non-negligible level of instability observed in the intervals preceding and following the swing phase for a considerable number of first steps. Consequently, the authors decided to exclude the first step from the algorithm's performance analysis. Following this procedure, the metrics were recalculated excluding the data from the first steps. The resulting values were: $E_{abs} = 0.0271$ m, $RMSE = 0.0337$ m, $E_{rel} = 2.45$ %, and $R^2 = 98.78$ %.

The new results were compared with the original baseline, Table 2, which included all steps. Table 2 shows that excluding data from the initial steps significantly enhances algorithm performance. This is evidenced by a reduction of over 10 % in the

E_{abs}, E_{rel}, and $RMSE$ metrics, indicating greater accuracy, and an increase of 0.5 % in the R^2 value, reflecting improved quality and consistency.

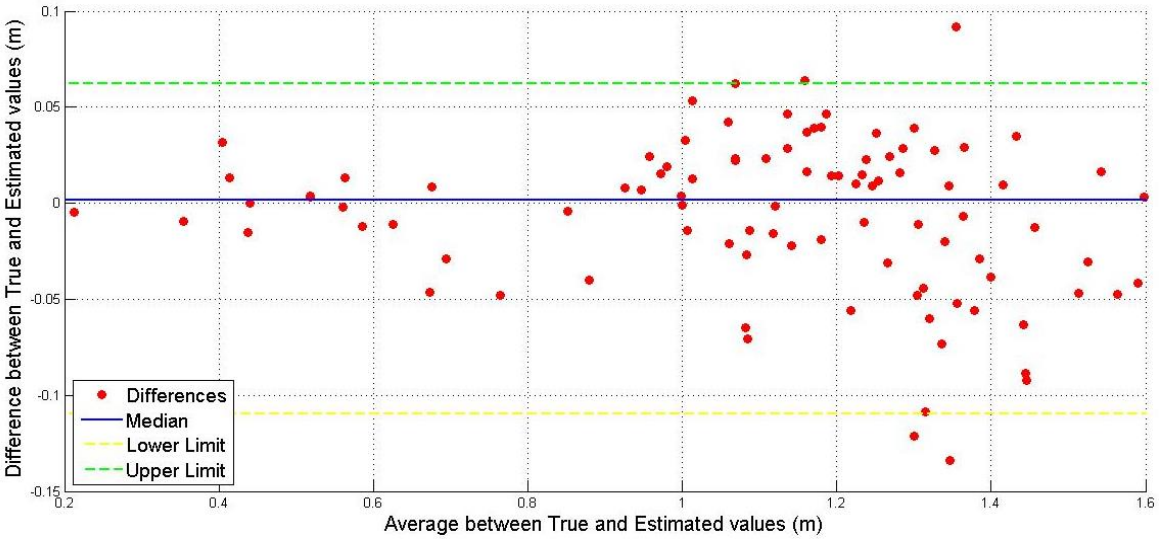

Figure 15

Bland-Altman Analysis

Table 2
Comparison of the performance of the proposed algorithm with the first steps and without the first steps

Performance Metrics	Including the First Steps	Excluding the First Steps	Improvement
E_{abs}	0.0313 m	0.0271 m	13.53 %
E_{rel}	0.0412 m	0.0337 m	18.14 %
$RMSE$	2.82 %	2.45 %	12.9 %
R^2	98.27 %	98.78 %	0.51 %

4.- CONCLUSIONS

This work proposed and validated a novel algorithm for stride length estimation. It is based on an analytical approach that leverages the specific characteristics of IMU signals when the wearable device is attached to the forefoot. The algorithm's implementation demonstrated its ability to provide accurate and reliable stride length estimates. According to the validation metrics, the proposed algorithm outperforms most results reported in prior studies. The final performance metrics were: $E_{abs} = 0.0313$ m, $RMSE = 0.0412$ m, $E_{rel} = 2.82$ %, and $R^2 = 98.27$ %.

Taken together, the applied statistical tests and inference methods establish that the stride length estimation algorithm exhibits robust performance from a statistical perspective. The absence of bias, the high agreement with the reference method, the stability of the error across changes in stride magnitude, and the consistency of the metrics indicate that the algorithm is accurate, precise, and stable, even in the presence of non-Gaussian distributed errors. Thus, this algorithm represents a significant contribution to recent efforts aimed at improving stride length estimation.

A key methodological aspect was the incremental increase of data used for validation. The gradual inclusion of data confirmed the sufficiency of the database and the robustness and reliability of the results.

It is worth mentioning that although the database was composed of IMU signals acquired under normal walking conditions, even though no restrictions were issued in this regard, the proposed method can be applied to any walking speed, provided that the stability time intervals corresponding to the foot stance phases are maintained.

A major strength of the algorithm is its analytical foundation, which provides a solid and reliable basis for estimation. This can be advantageous for diverse applications such as physical activity monitoring, sports performance tracking, and rehabilitation. By requiring a single IMU, the algorithm offers a more practical and cost-effective solution compared to more expensive alternatives. This combination of accuracy and affordability makes the proposed algorithm a highly suitable option for applications requiring stride length estimation.

Excluding the first step led to a significant performance improvement. This finding is relevant for applications that can omit the initial step without substantially degrading overall performance.

APPENDIX A

As explained in Section IV, a correction is applied to the gyroscope-derived angle measurements within the interval covering subphase 2 of the preceding stability phase, the swing phase, and the following stability phase (the total number of samples is denoted as N) to reduce the constant deviation affecting the gyroscope signal. This correction is based on the assumption that the average value of the rotation angles within the following stability phase, estimated from the gyroscope signals, should closely approximate the average value of the rotation angles within the same phase, as estimated from the accelerometer and magnetometer signals in the previous step.

The correction consists of applying a linear adjustment equal to $\frac{n}{N}\Delta$, where n is the sample index and Δ is a parameter chosen such that the mean of the gyroscope-estimated rotation angles within the following stability phase equals the mean of the corresponding angles estimated from the accelerometer and magnetometer signals. That is:

$$corrected\_angle(n) = ang_g(n) - \frac{n}{N}\Delta \tag{A.1}$$

The parameter Δ must ensure that the mean of the rotation angles within the following stability phase, estimated from the gyroscope signals, equals the mean of the corresponding angles estimated from the accelerometer and magnetometer signals. That is:

$$\overline{corrected\_angle_g} = \frac{\sum_{k=P+M+1}^{N} corrected\_angle_g(k)}{L} = Final\_Angle \tag{A.2}$$

where P is the number of samples in subphase 2 of the preceding stability phase, M is the number of samples in the swing phase, and L is the number of samples in the following stability phase.

Substituting Equation (A.1) into (A.2),

$$\overline{corrected\_angle_g} = \frac{\sum_{k=P+M+1}^{N} \left(ang_g(k) - \frac{k}{N}\Delta\right)}{L} = Final\_Angle \tag{A.3}$$

Solving Δ yields:

$$\sum_{k=P+M+1}^{N} ang_g(k) - \sum_{k=P+M+1}^{N} \frac{k}{N}\Delta = L \cdot Final\_Angle$$

$$\Delta \sum_{k=P+M+1}^{N} \frac{k}{N} = \sum_{k=P+M+1}^{N} ang_g(k) - L \cdot Final\_Angle$$

$$\Delta = \frac{\sum_{k=P+M+1}^{N} ang_g(k) - L \cdot Final\_Angle}{\sum_{k=P+M+1}^{N} \frac{k}{N}} \tag{A.4}$$

APPENDIX B

Since the effect of drift on the rotation angle estimation is not completely eliminated, the velocity obtained by integrating the acceleration signals and the subsequent displacement derived from this velocity will not be optimal. Considering that during the preceding and following stability phase intervals, the movement measured by the IMU is nearly null, the next step is to perform a two-step adjustment on the rotated acceleration signals.

The first adjustment is applied to the samples of the rotated acceleration signals (or later, to the velocity signals resulting from the integration of the adjusted accelerations) within the interval covering the swing phase and the following stability phase. The total number of samples in this interval is denoted as N_{a_1}. This adjustment consists of a linear correction to the signal values by a factor of $\frac{n}{N_{a_1}}\Delta_{a_1}$, where n is the sample index starting from the first sample of the swing phase ($n = 1$) and ending at the last sample of the following stability phase ($n = N_{a_1}$). That is:

$$adjusted\_signal(n) = signal(n) - \frac{n}{N_{a_1}}\Delta_{a_1} \tag{B.1}$$

The parameter Δ_{a_1} is determined such a way that the average of the adjusted signal samples within the following stability phase equals zero. That is:

$$\overline{adjusted\_signal} = \frac{\sum_{k=M+1}^{N_{a_1}} adjusted\_signal(k)}{L} = 0 \tag{B.2}$$

where M is the number of samples in the swing phase, and L is the number of samples in the following stability phase.

If equation (B.1) is substituted into (B.2),

$$\overline{adjusted\_signal} = \frac{\sum_{k=M+1}^{N_{a_1}} \left(signal(k) - \frac{k}{N_{a_1}}\Delta_{a_1} \right)}{L} = 0 \tag{B.3}$$

Solving Δ_{a_1} yields:

$$\sum_{k=M+1}^{N_{a_1}} signal(k) - \sum_{k=M+1}^{N_{a_1}} \frac{k}{N_{a_1}}\Delta_{a_1} = 0$$

$$\Delta_{a_1} \sum_{k=M+1}^{N_{a_1}} \frac{k}{N_{a_1}} = \sum_{k=M+1}^{N_{a_1}} signal(k)$$

$$\Delta_{a_1} = \frac{\sum_{k=M+1}^{N_{a_1}} signal(k)}{\sum_{k=M+1}^{N_{a_1}} \frac{k}{N_{a_1}}} \tag{B.4}$$

ACKNOWLEDGEMENTS

The paper received financial support from OGFPI, the Cuban Neuroscience Center, and the Technological University of Havana, Cujae.

REFERENCES

1. Wang, M.C.; Liao, W.C.; Lee, K.C.; Lu, S.H.; Lin, Y.P. Validation of Screening Tools for Predicting the Risk of Functional Decline in Hospitalized Elderly Patients. Int. J. Environ. Res. Public Health 2022, 19, 6685. https://doi.org/10.3390/ijerph19116685.

2. González Garcés, Y.; Rodríguez Labrada, R.; Torres Vega, R.; Velázquez Pérez, L. Métodos para la evaluación de la marcha y postura en pacientes con ataxias hereditarias. Anal. Acad. Cienc. Cuba 2022, 12, 2.
3. Feijó, F.; Bonezi, A.; Stefen, C.; Polero, P.; Bona, R.L. Evaluation of Older Adults with Functional and Walking Tests. Educ. Física Cienc. 2018, 20, 3.
4. Gao, H.; Frommelt, L.; Kasneci, E. The Evaluation of Gait-Free Locomotion Methods with Eye Movement in Virtual Reality. In Proceedings of the 2022 IEEE International Symposium on Mixed and Augmented Reality Adjunct (ISMAR-Adjunct), Singapore, 17–21 October 2022; pp. 530–535. https://doi.org/10.1109/ISMAR-Adjunct57072.2022.00112.
5. Kumar, N.; Kunju, N.; Kumar, A.; Sohi, B.S. Active Marker Based Kinematic and Spatio-Temporal Gait Measurement System Using LabVIEW Vision. J. Sci. Ind. Res. 2010, 69, 600–605.
6. Ekvall Hansson, E.; Akar, Y.; Liu, T.; et al. Gait Parameters When Walking with or Without Rollator on Different Surface Characteristics: A Pilot Study Among Healthy Individuals. BMC Res. Notes 2022, 15, 308. https://doi.org/10.1186/s13104-022-06196-9.
7. Bleser, G.; Taetz, B.; Miezal, M.; Christmann, C.A.; Steffen, D.; Regenspurger, K. Development of an Inertial Motion Capture System for Clinical Application: Potentials and Challenges from the Technology and Application Perspectives. i-com 2017, 16, 113–129. https://doi.org/10.1515/icom-2017-0010.
8. Castellanos-Ruíz, J.; Montealegre-Mesa, L.M.; Martínez-Toro, B.D.; Gallo-Serna, J.J.; Fuentes, O.A. Uso de Sensores Inerciales en Fisioterapia: Una Aproximación a Procesos de Evaluación del Movimiento Humano. Univ. Salud 2021, 23, 55–63. https://doi.org/10.22267/rus.212301.214.
9. Cismas, A.; Matei, I.; Ciobanu, V.; Casu, G. Crash Detection Using IMU Sensors. In Proceedings of the 2017 21st International Conference on Control Systems and Computer Science (CSCS), Bucharest, Romania, 29–31 May 2017; pp. 672–676. https://doi.org/10.1109/CSCS.2017.103.
10. Pérez Molinet, A.; Hernández Montero, F.E.; Arencibia Castellanos, G.; Rodriguez, J.R. Estimación de la Posición a Través de IMU Basada en la Detección de Periodos de Estabilidad Durante la Marcha. Orange J. 2021, 3, 16–29. https://doi.org/10.46502/issn.2710-995X/2021.5.03.
11. Jimenez, A.R.; Seco, F.; Prieto, C.; Guevara, J. A Comparison of Pedestrian Dead-Reckoning Algorithms Using a Low-Cost MEMS IMU. In Proceedings of the 2009 IEEE International Symposium on Intelligent Signal Processing, Budapest, Hungary, 26–28 August 2009; pp. 37–42. https://doi.org/10.1109/WISP.2009.5286542.
12. Sijobert, B.; Benoussaad, M.; Denys, J.; Pissard-Gibollet, R.; Geny, C.; Coste, C.A. Implementation and Validation of a Stride Length Estimation Algorithm, Using a Single Basic Inertial Sensor on Healthy Subjects and Patients Suffering from Parkinson's Disease. Health 2015, 7, 704–714. https://doi.org/10.4236/health.2015.76084.
13. Gu, F.; Khoshelham, K.; Yu, C.; Shang, J. Accurate Step Length Estimation for Pedestrian Dead Reckoning Localization Using Stacked Autoencoders. IEEE Trans. Instrum. Meas. 2019, 68, 2705–2713. https://doi.org/10.1109/TIM.2018.2871808.
14. Wang, Q.; Ye, L.; Luo, H.; Men, A.; Zhao, F.; Ou, C. Pedestrian Walking Distance Estimation Based on Smartphone Mode Recognition. Remote Sens. 2019, 11, 1140. https://doi.org/10.3390/rs11091140.
15. Wang, Q.; et al. Personalized Stride-Length Estimation Based on Active Online Learning. IEEE Internet Things J. 2020, 7, 5405–5413. https://doi.org/10.1109/JIOT.2020.2971318.
16. Sui, J.-D.; Chang, T.-S. IMU Based Deep Stride Length Estimation With Self-Supervised Learning. IEEE Sens. J. 2021, 21, 7380–7387. https://doi.org/10.1109/JSEN.2021.3049523.
17. Vezocnik, M.; Kamnik, R.; Juric, M.B. Inertial Sensor-Based Step Length Estimation Model by Means of Principal Component Analysis. Sensors 2021, 21, 3527. https://doi.org/10.3390/s21103527.
18. Suzuki, Y.; Hahn, M.E.; Enomoto, Y. Estimation of Foot Trajectory and Stride Length During Level Ground Running Using Foot-Mounted Inertial Measurement Units. Sensors 2022, 22, 7129. https://doi.org/10.3390/s22197129.
19. Zhou, J.; Mao, Q.; Yang, F.; Zhang, J.; Shi, M.; Hu, Z. Development and Assessment of Artificial Intelligence-Empowered Gait Monitoring System Using Single Inertial Sensor. Sensors 2024, 24, 5998. https://doi.org/10.3390/s24185998.

20. Zadka, A.; Rabin, N.; Gazit, E.; et al. A Wearable Sensor and Machine Learning Estimate Step Length in Older Adults and Patients with Neurological Disorders. npj Digit. Med. 2024, 7, 142. https://doi.org/10.1038/s41746-024-01136-2.
21. Burggräf, P.; Pérez Martínez, A.R.; Roth, H.; et al. Quadrotors in Factory Applications: Design and Implementation of the Quadrotor's P-PID Cascade Control System. SN Appl. Sci. 2019, 1, 722. https://doi.org/10.1007/s42452-019-0698-7.
22. P. A. M. Panchi and D. F. M. Panchi, "Pruebas estadísticas de normalidad: un análisis comparativo entre Kolmogórov-Smirnov, Shapiro-Wilk, Anderson-Darling, Ryan-Joiner Y Jarque-Bera," *CIENCIA UNEMI*, vol. 18, no. 49, Sept. 2025, doi: 10.29076/issn.2528-7737vol18iss49.2025pp%25pp.
23. T. Kesgin and R. İlayda, "Revisiting Trend Stability Using Mann-Kendall and Wilcoxon Signed-Rank Tests Through Innovative Method Comparisons," Sustainability, vol. 17, no. 23, p. 10454, Jan. 2025, doi: 10.3390/su172310454.
24. S. Haghayegh, H.-A. Kang, S. Khoshnevis, M. H. Smolensky, and K. R. Diller, "A comprehensive guideline for Bland–Altman and intra class correlation calculations to properly compare two methods of measurement and interpret findings," Physiol. Meas., vol. 41, no. 5, p. 055012, June 2020, doi: 10.1088/1361-6579/ab86d6.
25. S. F. Mokhtar, Z. M. Yusof, and H. Sapiri, "Confidence Intervals by Bootstrapping Approach: A Significance Review," Malaysian Journal of Fundamental and Applied Sciences, vol. 19, no. 1, pp. 30–42, Feb. 2023, doi: 10.11113/mjfas.v19n1.2660.

CONFLICT OF INTEREST AND AUTHOR RESPONSIBILITY STATEMENTS

The authors declare no conflicts of interest with any institution, organization, or entity that could influence or bias the work presented in this manuscript. The research was conducted in the absence of any commercial or financial relationships that could be construed as a potential conflict of interest.

The views and opinions expressed in this article are solely those of the authors and do not necessarily reflect the official policy or position of any affiliated institution or funding agency.

AUTHOR CONTRIBUTIONS:

Fidel Hernandez: Conceptualization, Methodology, Investigation, Writing—original draft preparation, project administration **Melissa Domínguez:** Conceptualization, Methodology, Investigation, Software, **Brenda Guitard:** Conceptualization, Methodology, Investigation, Software, Data curation **René Corvo:** Investigation, Software, Validation **Jon Altuna:** Validation, Resources, Writing—review and editing, Funding acquisition.

AUTHORS:

Fidel Hernandez: Eng. on Telecommunications and Electronics, PhD, Faculty of Telecommunications and Electronics Engineering, Technological University of Havana, Cuba; fhernandez@tele.cujae.edu.cu, ORCID: 0000-0002-5003-2807. Research interests include machine condition monitoring and diagnostics, and inertial sensor-based wearable devices for human activity monitoring.

Melissa Domínguez: Eng. on Telecommunications and Electronics, Faculty of Telecommunications and Electronics Engineering, Technological University of Havana, Cuba; melisdomcab@tele.cujae.edu.cu, ORCID: 0000-0001-7158-0776. Research interests include inertial sensor-based wearable devices for human activity monitoring.

Brenda Guitard: Eng. on Telecommunications and Electronics, Faculty of Telecommunications and Electronics Engineering, Technological University of Havana, Cuba; bcguival@gmail.com, ORCID: 0009-0006-1015-7265. Research interests include inertial sensor-based wearable devices for human activity monitoring.

René Corvo: Eng. on Telecommunications and Electronics, Faculty of Telecommunications and Electronics Engineering, Technological University of Havana, Cuba; recorvo02@gmail.com, ORCID: 0009-0000-2973-8779. Research interests include inertial sensor-based wearable devices for human activity monitoring.

Jon Altuna: Eng. on Electronics and Industrial Automation, PhD, Mondragon Unibersitatea, Spain; jaltuna@mondragon.edu, ORCID: 0009-0009-4883-7540. Research interests include machine condition monitoring and diagnostics, and inertial sensor-based wearable devices for human activity monitoring.